

Design for minimizing fracture risk of all-ceramic cantilever dental bridge

Zhongpu Zhang^a, Shiwei Zhou^b, Eric Li^a, Wei Li^a, Michael V. Swain^c and Qing Li^{a,*}

^a*School of Aerospace, Mechanical and Mechatronic Engineering, The University of Sydney, Sydney, NSW 2006, Australia*

^b*Centre for Innovative Structures and Materials, School of Civil, Environmental and Chemical Engineering, RMIT University, GPO Box 2476, Melbourne 3001, Australia*

^c*Disciplines of Biomaterials, Faculty of Dentistry, The University of Sydney, NSW 2010, Australia*

Abstract. Minimization of the peak stresses and fracture incidence induced by mastication function is considered critical in design of all-ceramic dental restorations, especially for cantilever fixed partial dentures (FPDs). The focus of this study is on developing a mechanically-sound optimal design for all-ceramic cantilever dental bridge in a posterior region. The topology optimization procedure in association with Extended Finite Element Method (XFEM) is implemented here to search for the best possible distribution of porcelain and zirconia materials in the bridge structure. The designs with different volume fractions of zirconia are considered. The results show that this new methodology is capable of improving FPD design by minimizing incidence of crack in comparison with the initial design. Potentially, it provides dental technicians with a new design tool to develop mechanically sound cantilever fixed partial dentures for more complicated clinical situation.

Keywords: Fixed partial dentures (FPDs), cantilever bridge, topology optimization, Extended Finite Element Method (XFEM), fracture mechanics

1. Introduction

All-ceramic dental bridge, or namely fixed partial denture (FPD), has been used for many years to replace missing teeth attributable to its outstanding aesthetics and excellent biocompatibility [1, 2]. However, using it for a cantilever structure is still questionable in clinic due to their weak structural strength especially in the case of posterior region [3, 4]. Although implantation becomes increasingly popular and favorable in treating such a group of patients, it may be restricted due to quantity and quality of surrounding bone, cost and other complications. In order to overcome the above-mentioned strength problem, zirconia has proven one of the most appropriate choices used as a framework material to improve mechanical characteristics in all-ceramic dental bridges. Nevertheless, it remains challenging for dental technicians or clinicians to figure out what is the best possible allocation of porcelain and zirconia materials for the abovementioned dental bridge structures.

* Address for correspondence: Qing Li, School of Aerospace, Mechanical and Mechatronic Engineering, The University of Sydney, Sydney, NSW 2006, Australia. Tel.: 612-93518607; Fax: 612-93517060; E-mail: qing.li@sydney.edu.au.

A number of relevant studies on FPDs have focused on technical complications, fracture mechanism and stress peaks within the prosthetic devices. In the all-ceramic three-unit FPDs, the highest stresses were found at the gingival region of the connector [5], where crack could be likely initiated from and propagated toward the loading point in the center of the pontic [6, 7]. The model with a greater radius at the gingival embrasure exhibited a lower stress concentration. The average failure load increased by 140% if the radius at gingival embrasure increased from 0.25 to 0.9 mm [5]. However, the curvature at occlusal embrasure had little effect on the fracture resistance of the three-unit FPD. Structurally, it remains largely under-studied how to reduce the risk of fracture incidence by optimizing topological configurations of different ceramic materials in a systematic manner.

This study aims to combine the topology optimization technique with fracture analysis using the extended finite element method (XFEM) for the design of three-unit cantilever bridges. On one hand, topology optimization has proven a rather powerful design tool to determine an optimal distribution of a prescribed amount of materials under different load cases within a given design domain [8]. Much effort has been devoted to the advances in modern topology optimization algorithms over the last three decades, and topology optimization has been extensively used in a wide range of engineering problems recently [9]. On the other hand, crack initiation and propagation in dental bridges can be modeled using continuum-to-discrete element method (CDEM) [10-13] or XFEM which signifies numerical techniques particularly suitable to the simulation of crack initiation and propagation in an automatic fashion [14]. XFEM has been used successfully in biomechanical applications recently [15-18]. One of the advantages of XFEM is that the finite element (FE) mesh can be created independently of any possible cracking geometry, where remeshing operation is not required to track the cracking path precisely [19]. Lured by such features, XFEM is considered particularly suitable to be integrated into topology optimization in a fixed grid FE framework.

Unlike traditional topology optimization that uses standard FEM, this study proposes to employ XFEM for topology optimization to enhance fracture resistance in all-ceramic cantilever dental bridges. The optimized designs will be of lower risk of fracture, thereby potentially improving the longevity of all-ceramic dental prostheses from an engineering perspective.

2. Materials and methods

2.1 Finite element modeling

A set of micro-CT (computerized tomography) images of human mandible section was used for capturing the geometry of bone segments and tooth structures. The finite element models were constructed using image processing program ScanIP (Simpleware Pty Ltd) and solid modeling software SolidWorks 2012 (Dassault Systèmes Solidworks Corp.). A three-unit cantilever bridge was constructed for replacing a missed second premolar tooth as shown in Figure 1.

The bridge considered here is of an onlay configuration [18]. The model comprised two adjacent teeth as abutments, dentine, pulp, periodontal ligament (PDL), cortical bone and cancellous bone as native tissues. In this study, 2D plane stress models were considered for a demonstrative purpose [13], which was meshed in four-node quadrilateral elements with a global size of 0.2 mm. A convergence test was conducted to ensure that reduction of mesh size is insignificant to mechanical responses [20, 21].

In this study, all the materials were assumed as isotropic, homogeneous and linear elastic as used in numerous previous fracture analyses [11-13] (Table 1). The pressure distributed equivalent to a total

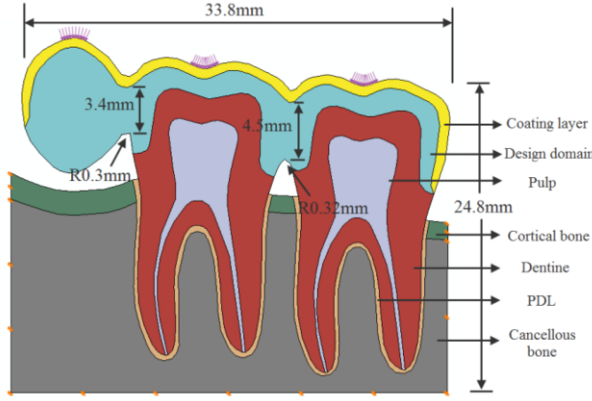


Fig. 1. FE model of a three-unit cantilever FPD.

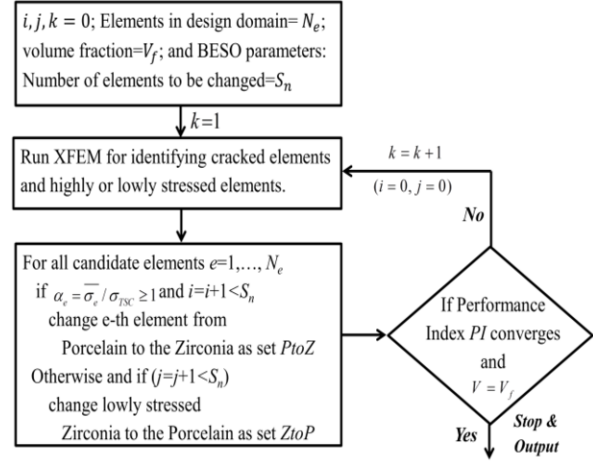


Fig. 2. Flowchart of the BESO algorithm.

Table 1

Mechanical properties of materials are used in this study [23, 24]

Materials	Young's modulus E (GPa)	Poisson's ratio ν	Tensile strength σ_{TS} (GPa)	Strainenergy release rate G_c (J/m ²)
Porcelain	69	0.26	0.045	13.3
Zirconia	210	0.32	0.44	144
Dentine	18	0.31		
Pulp	0.01	0.49		
PDL	0.0703	0.45		
Cortical bone	13.7	0.3		
Cancellous bone	1.37	0.32		

force of 250 N was applied to the central fossa of the pontic and two adjacent teeth as shown in Figure 1. In the FE analysis, the load was increased linearly over the defined time duration of one second until fracture occurred. The boundary of bone segments was kinematically fixed [11, 13]. The average thickness of the veneering ceramics was set to be 0.5mm for ensuring good aesthetic appearance [22].

2.2 Description of XFEM

In this paper, the criterion of maximum principal stress-based damage initiation was adopted. The FE formulation is enriched by the additional shape functions using partition of unity as follows [25],

$$u^h(x) = \sum_{i \in I} u_i N_i(x) + \sum_{i \in I} a_i N_i(x) H(x) + \sum_{i \in I} N_i(x) \left(\sum_{l=1}^4 b_l^i F_l(x) \right) \quad (1)$$

where I is the set of nodes in the mesh, u_i is the conventional degree of freedom at node i . N_i is the shape function associated with node i . $I \subset I$ is the subset of nodes enriched by the Heaviside function $H(x)$. The functions $F_l(x)$, $l = 1, \dots, 4$ are used for modeling the crack tip given as

$$\{F_l(x)\} = \left\{ \sqrt{r} \sin\left(\frac{\theta}{2}\right), \sqrt{r} \cos\left(\frac{\theta}{2}\right), \sqrt{r} \sin\left(\frac{\theta}{2}\right) \sin(\theta), \sqrt{r} \cos\left(\frac{\theta}{2}\right) \sin(\theta) \right\} \quad (2)$$

In the XFEM fracture modeling, crack could take place from the element with the high tensile stress. When the maximum principal stress reaches a predefined tensile strength of the material (i.e. 45MPa for the porcelain and 440MPa for the zirconia, respectively [15]), crack initiates in such completely-damaged elements. Then the crack propagates for releasing energy [25], for which the strain energy release rate (Table 1) was used here [26]. In the homogeneous medium, the crack will propagate in the direction perpendicular to the maximum principal stress.

2.3 Description of topology optimization method

In this study, the objective of topology optimization was to prevent the structure from cracking by designing mechanically strong multilayer all-ceramic configuration for the cantilever FPD structure. To make the material usage fully functional for fracture resistance, the overall performance index (PI) is defined in terms of elemental PI as its peak tensile stress to the fracture strength α^e as follows:

$$\min PI = \frac{1}{N_C} \sum_{e_c=1}^{N_C} [\alpha^{e_c}]^{p_c} + \frac{1}{N_Z} \sum_{e_z=1}^{N_Z} [\alpha^{e_z}]^{p_z} = \sum_{e_c=1}^{N_C} \left[\frac{\sigma_1^{e_c}}{\sigma_{TSC}} \right]^{p_c} + \sum_{e_z=1}^{N_Z} \left[\frac{\sigma_1^{e_z}}{\sigma_{TSZ}} \right]^{p_z} \quad (3)$$

where $\sigma_1^{e_c}$ is the first principal stresses in porcelain, $\sigma_1^{e_z}$ is the first principal stresses in zirconia, σ_{TSC} is the tensile strength of porcelain and σ_{TSZ} is the tensile strength of zirconia.

Since stress criterion was involved, the non-gradient bidirectional evolutionary structural optimization (BESO) method was employed. The basic idea is to start from an initial porcelain-only design; and then gradually replace fractured or weaker porcelain material by using stronger zirconia material until the PI is minimized (Figure 2). More details about BESO the algorithm can be consulted from the literature [27].

3. Results and discussion

The peak principal stress distribution in the three-unit cantilever bridge prior to fracture is exhibited in Figure 3(a). The peak principal stress in the three-unit cantilever bridge occurred at the occlusal embrasure between pontic and the first molar as circled in Figure 3(a). The region with a high-stress concentration in the model could be a potential site of damage and crack initiation [15].

The fracture pattern of the initial design is shown in Figure 3(b), in which the crack initiated at the occlusal embrasure and propagated perpendicularly to the gingival embrasure between the pontic and the first molar. Note that the fracture pattern predicted by XFEM showed good agreement with clinical recommendation that gingival embrasure must be prepared carefully for multi-unit FPDs.

Using the BESO procedure, Figure 4 shows the optimization histories of the performance index evolution vs BESO iteration. As more and more porcelain material was replaced by zirconia in the optimization (see the corresponding topological variation, where porcelain was plotted in light blue and zirconia in dark blue), the objective PI decreased gradually. From the inserts of topological

(Figure 4), the cracks were observed in the early stage, where objective PI increased. But it decreased smoothly when no cracks occurred after iteration 9. Note that the final convergent optimum was obtained at iteration 90 with a given volume fraction (30%).

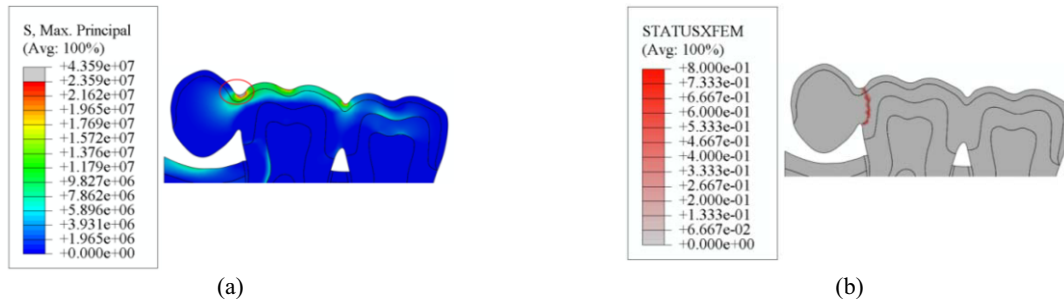


Fig. 3. (a) first principal stress contour within three-unit cantilever bridge structure; and (b) fracture site and cracking path.

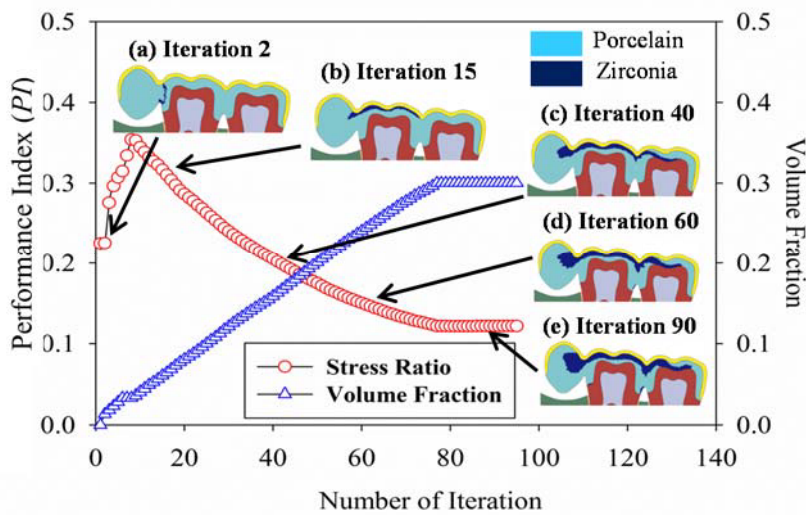



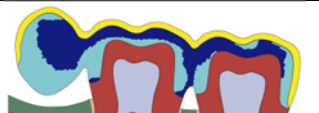


Fig. 4. The histories of the objective performance index (PI) and volume fraction for the three-unit cantilever bridge: (a) iteration 2, (b) iteration 15, (c) iteration 40, (d) iteration 60, and (e) final optimized topology at iteration 90.

Table 2

The optimal configurations of cantilever dental bridge under different constraints of volume fractions

Volume fraction at 20%	Volume fraction at 30%
	
Volume fraction at 40%	Volume fraction at 50%
	

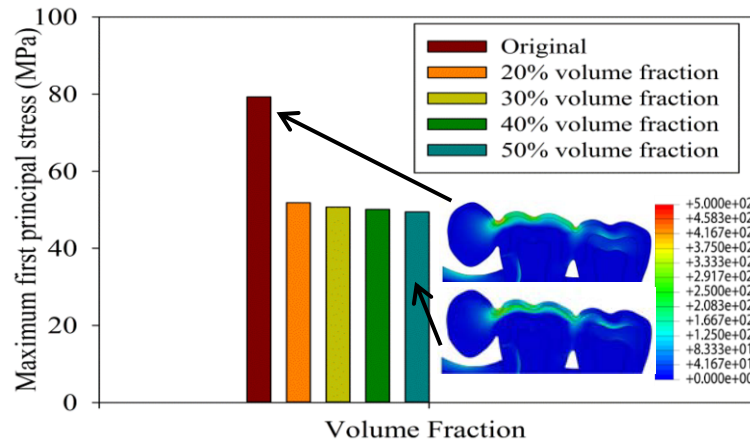


Fig. 5. The peak first principal stress of various optimized designs with different volume fractions.

Table 2 summarizes the final optimum designs of the three-unit cantilever bridge subject with different volume fractions at $V_f=20\%$, 30% , 40% and 50% , respectively. It is seen that the zirconia material was gradually added to the areas of occlusal embrasure between the pontic and two abutments.

The topology optimization adopted here implemented the fracture-mechanics-driven XFEM to search the best possible allocation of ceramic materials for the posterior cantilever dental bridge. This allows simulating the cracking and modeling fracture path in an automatic fashion. The results showed that the peak tensile stress substantially decreased in the optimal design in comparison with the initial design as shown in Figure 5. The novel topological designs (Table 2) may be implemented using additive manufacturing technology of ceramic and followed by a proper sintering process.

Predictability of such mechanically weak FPD structures as the cantilever bridge indicates a key feature in the design and fabrication of dental prostheses. XFEM provides an effective tool to simulate crack initiation and propagation, which has been well integrated into topology optimization procedure here. It has been shown that the optimal design of layered ceramic FPD configuration potentially reduces the onsite of fracture failure, thereby enhancing its longevity of treatment.

4. Conclusion

In this study, the topology optimization technique was combined with the extended finite element method (XFEM) to search the best possible bi-material configuration for enhancing fracture resistance. Through the non-gradient bidirectional evolutionary structural optimization (BESO) procedure, the cracked weak porcelain material in the highly stressed region was gradually replaced with strong zirconia material. As a result, all the cracked sites were eliminated from the structure and the fracture resistance is enhanced. The proposed XFEM based topology optimization technique can be extended to other designs of prosthetic devices, where fracture is a main concern.

Acknowledgment

The support from the Australian Research Council (ARC) is greatly acknowledged.

References

- [1] M. Guazzato, K. Proos, L. Quach and M.V. Swain, Strength, reliability and mode of fracture of bilayered porcelain/zirconia (Y-TZP) dental ceramics, *Biomaterials* **25** (2004), 5045–5052.
- [2] I. Sailer, B.E. Pjetursson, M. Zwahlen and C.H.F. Haemmerle, A systematic review of the survival and complication rates of all-ceramic and metal-ceramic reconstructions after an observation period of at least 3 years, Part II: fixed dental prostheses, *Clinical Oral Implants Research* **18** (2007), 86–96.
- [3] H. Fischer, M. Weber and R. Marx, Lifetime prediction of all-ceramic bridges by computational methods, *Journal of Dental Research* **82** (2003), 238–242.
- [4] P.M. Patel, C.D. Lynch, A.J. Sloan and A.S.M. Gilmour, Treatment planning for replacing missing teeth in UK general dental practice: current trends, *Journal of Oral Rehabilitation* **37** (2010), 509–517.
- [5] W. Oh, N. Gotzen and K.J. Anusavice, Influence of connector design on fracture probability of ceramic fixed-partial dentures, *Journal of Dental Research* **81** (2002), 623–627.
- [6] B. Taskonak, J.J. Mecholsky and K.J. Anusavice, Fracture surface analysis of clinically failed fixed partial dentures, *Journal of Dental Research* **85** (2006), 277–281.
- [7] W. Kou, S.Q. Kou, H.Y. Liu and G. Sjogren, Numerical modeling of the fracture process in a three-unit all-ceramic fixed partial denture, *Dental Materials* **23** (2007), 1042–1049.
- [8] O. Sigmund and K. Maute, Topology optimization approaches, *Structural and Multidisciplinary Optimization* **48** (2013), 1031–1055.
- [9] J.K. Guest, Imposing maximum length scale in topology optimization, *Structural and Multidisciplinary Optimization* **37** (2009), 463–473.
- [10] I. Ichim, Q. Li, J. Loughran, M.V. Swain and J. Kieser, Restoration of non-carious cervical lesions-Part I. Modelling of restorative fracture, *Dental Materials* **23** (2007), 1553–1561.
- [11] I. Ichim, Q. Li, W. Li, M.V. Swain and J. Kieser, Modelling of fracture behaviour in biomaterials, *Biomaterials* **28** (2007), 1317–1326.
- [12] I.P. Ichim, P.R. Schmidlin, Q. Li, J.A. Kieser and M.V. Swain, Restoration of non-carious cervical lesions-Part II. Restorative material selection to minimise fracture, *Dental Materials* **23** (2007), 1562–1569.
- [13] Q. Li, I. Ichim, J. Loughran, W. Li, M. Swain and J. Kieser, Numerical simulation of crack formation in all ceramic dental bridge, in: *Fracture of Materials: Moving Forwards*, H.Y. Liu, X. Hu and M. Hoffman, eds., 2006, pp. 293–298.
- [14] W. Li, C. Rungsiyakull, Z. Zhang, S. Zhou, M. Swain, I. Ichim and Q. Li, Computational fracture modelling in bioceramic structures, *Advanced Materials Research* **268–270** (2011), 853–856.
- [15] Z.P. Zhang, M. Guazzato, T. Sornusuwan, S.S. Scherrer, C. Rungsiyakull, W. Li, M.V. Swain and Q. Li, Thermally induced fracture for core-veneered dental ceramic structures, *Acta Biomaterialia* **9** (2013), 8394–8402.
- [16] I.V. Singh, B.K. Mishra, S. Bhattacharya and R.U. Patil, The numerical simulation of fatigue crack growth using extended finite element method, *International Journal of Fatigue* **36** (2012), 109–119.
- [17] A.A. Ali, L. Cristofolini, E. Schileo, H. Hu, F. Taddei, R.H. Kim, P.J. Rullkoetter and P.J. Laz, Specimen-specific modeling of hip fracture pattern and repair, *Journal of Biomechanics* **47** (2014), 536–543.
- [18] M.C. Thompson, Z. Zhang, C.J. Field, Q. Li and M.V. Swain, The all-ceramic, inlay supported fixed partial denture, Part 5, Extended finite element analysis validation, *Australian Dental Journal* **58** (2013), 434–441.
- [19] T. Belytschko and T. Black, Elastic crack growth in finite elements with minimal remeshing, *International Journal for Numerical Methods in Engineering* **45** (1999), 601–620.
- [20] W. Li, M.V. Swain, Q. Li, J. Ironside and G.P. Steven, Fibre reinforced composite dental bridge, Part II: Numerical investigation, *Biomaterials* **25** (2004), 4995–5001.
- [21] W. Li, M.V. Swain, Q. Li and G.P. Steven, Towards automated 3D finite element modeling of direct fiber reinforced composite dental bridge, *Journal of Biomedical Materials Research Part B–Applied Biomaterials* **74B** (2005), 520–528.
- [22] O. Ozturk, B. Uludag, A. Usumez, V. Sahin and G. Celik, The effect of ceramic thickness and number of firings on the color of two all-ceramic systems, *Journal of Prosthetic Dentistry* **100** (2008), 99–106.
- [23] S.S. Scherrer, J.R. Kelly, G.D. Quinn and K. Xu, Fracture toughness (K_{Ic}) of a dental porcelain determined by fractographic analysis, *Dental Materials* **15** (1999), 342–348.
- [24] Z. Zhang, S. Zhou, Q. Li, W. Li and M.V. Swain, Sensitivity analysis of bi-layered ceramic dental restorations, *Dental Materials* **28** (2012), E6–E14.
- [25] E. Giner, N. Sukumar, J.E. Tarancon and F.J. Fuenmayor, An Abaqus implementation of the extended finite element method, *Engineering Fracture Mechanics* **76** (2009), 347–368.
- [26] ABAQUS, 'ABAQUS Documentation', Dassault Systèmes, Providence, RI, USA, 2011.
- [27] X. Huang and M. Xie, *Evolutionary Topology Optimization of Continuum Structures: Methods and Applications*, John Wiley & Sons, Chichester, England, 2010.